PREDICTING THE EVOLUTION OF PRESSURE ULCERS

Francisco J. Veredas, Héctor Mesa

Dpto. Lenguajes y Ciencias de la Computación, Universidad de Málaga, Málaga, Spain

Juan C. Morilla

Distrito Sanitario de Málaga, Servicio Andaluz de Salud, Málaga, Spain

Laura Morente

Escuela Universitaria de Enfermería, Diputación Provincial, Málaga, Spain

Keywords: Pressure ulcer, Wound, Prediction, Machine learning, Artificial intelligence.

Abstract: A pressure ulcer is a clinical pathology of localized damage to the skin and underlying tissue caused by pressure, shear or friction. Diagnosis, treatment and care of pressure ulcers are costly for health services. Accurate wound evaluation is a critical task for optimizing the efficacy of treatment and care. Prediction of wound evolution helps the effective management of health resources and planning of pharmacological treatment and health-care decisions. In this paper, different machine learning approaches have been designed and used to predict the evolution of pressure ulcers. These predictive systems are based on local features extracted from wound images which were weekly taken in uncontrolled lighting conditions. The images were automatically segmented by the mean-shift procedure. A group of clinical experts manually classified the segmented regions into five different tissue types, and a set of local descriptors based on area measurements of these tissues was extracted. The one-week evolution of two different indicators for pressure ulcer evaluation is predicted: the ratio between granulation and devitalized tissue, and the percentage of wound-bed border consisting of granulation tissue. Of the tens of machine learning approaches and architectures tested in this study, support vector machines, naive Bayes classifiers, neural networks and decision trees achieved the highest accuracy rates in the prediction of the two indicators above, with also acceptable sensitivity and positive predictive value rates. Feature selection significantly reduced the number of input features needed for prediction. Neural networks and decision trees gave the best performance results, and the C4.5 algorithm achieved the highest accuracy rate ($\sim 81\%$) in the prediction of the granulation/devitalized ratio from a small number of input features.

1 INTRODUCTION

The European Pressure Ulcer Advisory Panel (EPUAP) defines a pressure ulcer (PU) as an area of localized damage to the skin and underlying tissue caused by pressure, shear, friction and or a combination of these (European Pressure Ulcer Advisory Panel (EPUAP), 1999; Gawlitta et al., 2007). The prevention, care and treatment of PU pathology involve high costs for health services (Stratton et al., 2003) and imply important consequences for the health of the population. The prevalence of pressure ulcer varies in different contexts. Diverse studies carried out among different populations of patients

with home-care assistance or in acute care or long-term units have produced prevalence rates ranging from 7% to 33% (Zulkowski, 1999; Horn et al., 2002; Gunningberg, 2004; Tannen et al., 2004; Woodbury and Houghton, 2004). In a recent study, Landi *et al.* (Landi et al., 2007) have evidenced that PUs are associated with increased mortality rates, and Redelings *et al.* (Redelings et al., 2005) have reported PUs as a cause of death among 114,380 persons in the United States between 1990 and 2001.

Precise evaluation of PUs constitutes a crucial task for diagnosing, monitoring the evolution, and deciding on care intervention and pharmacological treatment to be arranged for each particular case. Clini-

cians evaluate and register the state of each PU using classification systems (Kottner et al., 2009) which are mainly based on the subjective visual inspection of the wound. These systems aim at providing consistent and accurate PU assessment that facilitates accurate communication, precise documentation and health-care decisions. Nevertheless, PU classification alone is not sufficient to decide on pharmacological treatment or health-care to be provided, and more accurate and sensitive monitoring of the PU healing evolution is therefore needed. One of the most widespread tools being used to determine the healing status of a PU is the PUSH (Pressure Ulcer Scale for Healing) tool (National Pressure Ulcer Advisory Panel et al., 2001), which is based on the visual detection of four main tissue types —i.e. epithelial, granulation, slough or necrosis (Sussman and Bates-Jensen, 2001)— together with the manual "gross" estimation of the wound area and the subjective perception of oozing from the ulcer. Recent prospective studies evaluating the PUSH tool, conclude that it can accurately differentiate between healed and non-healed ulcers, but some critical modifications must be done to improve its value and sensitivity to PU changes (Günes, 2009).

Recently, new principles have emerged which provide a systematic approach to the management of wounds. The International Advisory Board on Wound Bed Preparation has proposed TIME (Dowsett, 2008) as a new paradigm for wound management that is based on intervention in four clinical parameters: tissue (T) non-viable or deficient, infection or inflammation (I), moisture (M) imbalance, and epidermal (E) margin. Considering the histology and physiology of wound healing (Edsberg, 2007), parameters T and E of TIME framework could suffice to have an approach to wound healing state, so that I and M variables can directly be derived from the observation of T and E. Granulation tissue (a fibrous connective reddish tissue) is an indicator of the growth of new tissue during wound healing: as the PU heals, devitalized tissue (a yellowish oozing tissue caused by infection, or a blackish necrotic tissue) is progressively replaced with granulation tissue growing from the wound-bed center to the periphery so that, finally, granulation tissue reaches the wound-bed border and therefore fills the whole wound-bed; then, the PU starts closing (Sussman and Bates-Jensen, 2001). Thus, parameter T of TIME paradigm regards to the proportion of devitalized areas with respect to granulation tissue in the wound-bed, whereas parameter E becomes an estimator of the likelihood of epithelial cells to migrate from the wound-bed perimeter to the wound-bed center during the epitelization process: this migration re-

quires granulation tissue to cover the wound-bed and reach the wound-bed border with a highly vascularized layer. Therefore, proliferation of granulation tissue from the wound-bed center to the periphery directly implies the reduction of infection, inflammation and oozing from the wound. Furthermore, as other authors recently addressed, more accurate pressure ulcer evaluation and monitoring of the healing stage could be achieved by measuring and precisely locating all tissue types present in the wound or in its surrounding areas (Veredas et al., 2009). Suppose these measurements are computed and the significant tissues are located, new sensitive and precise indicators for evaluating the wound state can be designed.

Based on those new principles for the management of wounds above, in this study PU digital images have been taken, preprocessed and segmented, and computer assisted marking and tissue classification have been done by expert clinicians. Our computer-based image-processing strategy has been used to obtain two new sensitive indicators of the wound healing state which are closely connected with parameters T and E of TIME paradigm: 1) the ratio granulation/devitalized tissue, and 2) the proportion of the wound-bed border consisting of granulation tissue. Subsequently, we have used diverse machine-learning (ML) approaches to design predictive systems to independently predict the sign of the evolution, in one-week interval, of these two indicators above. As histological and clinical studies shown, increase of either the granulation/devitalized ratio or the proportion of granulation tissue in the wound-bed border reveals significant clinical improvement of the PU global state (Sussman and Bates-Jensen, 2001; Dowsett, 2008). Predicting the positive or negative tendency of these changes in the proportion and location of PU tissues helps the effective management of health resources and planning of pharmacological treatment and health-care decisions.

2 METHODOLOGY

Our methodology to predict the evolution of PUs is based on local features obtained from PU digital color images. These images had to be firstly acquired and subsequently processed, segmented and labeled to obtain precise area measurement of all significant tissues and regions present in the wound. These features are subsequently used to design predictive systems to forecast the evolution of the PU for a time interval of a week. Different ML approaches have been used in this study to design these predictive systems, with different performance rates obtained.

2.1 Image Acquisition and Processing

A sample of 69 sacrum and hip PUs (stages III and IV) from patients with home-care assistance (mean age 80.5 ± 12.3 years) was weekly photographed, registered and assessed until healing, transfer, patient death, or end of study for a maximum of 16 weeks. These PUs were photographed in uncontrolled lighting conditions using a Sony Cybershot® W30 digital camera. The images were taken with a flashlight to obtain the best quality images possible, and at a distance of approximately $30 - 40\,cm$ from the wound plane. To minimize the margin of error, the camera lens is oriented in parallel to the plane of the wound. Macro-focusing was used to ensure well-focused pictures within these short distances. A $1\,cm^2$-sized normalized white square paper patch was placed on the right top corner of each picture, which is used to estimate the dimensions of the wound and tissues. A total 743 photographs were finally obtained.

Our methodology for PU evaluation is based on the detection and measurement of the area of the most significant tissue types in the PU, i.e. skin, healing, granulation, slough and necrosis. The PU images acquired were automatically segmented using a segmentation technique known as mean shift procedure (Comaniciu and Meer, 2002). The mean shift has demonstrated to be a very reliable approach to image segmentation and has shown its efficiency in many vision tasks (Comaniciu and Meer, 2002) such us wound image segmentation (Wannous et al., 2007; Veredas et al., 2009). PU images show very heterogeneous colorations, imprecise and vague boundaries, which make most image segmentation techniques fail. For this reason, PU segmentation benefits from the main characteristic of the mean shift approach: the preservation of the borders of the regions resulting from the segmentation process. In our study, a mean of 150 regions per image were obtained from the application of the mean shift segmentation approach to the set of 743 PU images.

For this work, an *ad hoc* graphical user interface (called *PULAB, Pressure Ulcer LABoratory*) was specifically developed to deal with the wearisome task of "manually" labeling the whole set of regions from the segmented wound images (Veredas et al., 2009). PULAB software resulted from a previous phase of this same research project, and internally consists of a computational intelligence core based on a ML hybrid-learning approach to automatically recognize PU tissues in segmented PU images, with high accuracy rates. PULAB has been used to have an initial approach to tissue classification in the 743 images of this study. Subsequently, a collaborative group of 5 expert clinicians from the *Health Service of Málaga Province* supervised that classification and assigned the definitive label —i.e. skin, healing, granulation, slough and necrosis— to each one of the segmented regions in the images. For each segmented region, its final label was assigned by a voting process, so that the tissue class with the largest number of votes was assigned to that segmented region. For some unclear or ambiguous regions, some later discussion was required to achieve a final agreement on the tissue type those regions consisted of. This way, precise tissue classification for PU evaluation is achieved. The $1\,cm^2$ square marker is also detected in each image and labeled by the experts, and it is subsequently used to convert the tissue area measures from pixel units to standard measurement units (mm^2). PULAB software dramatically reduced the time consumed during the wearisome process of marking and classifying the segmented regions in the images. Figure 1 shows an example of a PU ulcer image of our study which has been automatically segmented and manually labeled by the group of expert clinicians.

From these labeled regions in the images, the area of each of the PU tissue types is measured and expressed in standard units by using the normalized square marker. This way, the area of skin, healing tissue, necrosis, slough, granulation and wound-bed (i.e. granulation + slough + necrosis) can be calculated. These area measures and their combinations (see next section) are the variables used in the design of the predictive systems for PU evolution based on ML approaches.

2.2 Pressure Ulcer Local Features

The initial set of local PU features consists of 46 features and includes three different types of characteristics obtained from the analysis of the distribution of the tissue types in the ulcer: *absolute*, *relative*, and *differential descriptors*.

Absolute features are the areas of the different tissue types and significant regions in the image: healing tissue (A_{heal}), granulation (A_{gran}), slough (A_{slough}), necrosis (A_{nec}), wound-bed (A_{wound}), i.e. granulation + slough + necrosis, and the entire PU (A_{pu}), i.e. wound-bed + healing tissue, in squared millimeters, calculated by approximating the area of the tissues from the measurement of the reference area of the $1\,cm^2$-sized square marker.

Relative descriptors are obtained by considering the relative distribution of the tissues in the wound-bed and the perimeter of the wound-bed:

- Proportion of granulation ($P_{gran} = A_{gran}/A_{wound}$), slough ($P_{slough} = A_{slough}/A_{wound}$), necrosis ($P_{nec} =$
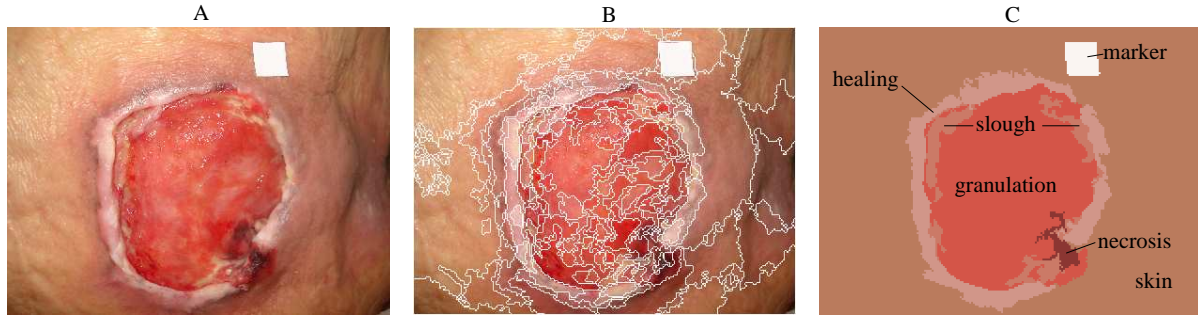
Figure 1: Example of region segmentation (figure B) and labeling (figure C) for a PU image (the original unprocessed image is shown in A). In figure C, all the regions with the same label (i.e. the same tissue type) are given a similar pseudo-color that is calculated as an average of the colors from these regions in the image.

A_{nec}/A_{wound}) and devitalized tissues ($P_{dev} = A_{dev}/A_{wound}$), i.e. slough and necrosis, in the wound-bed.

- Percentage of the wound-bed perimeter consisted of granulation tissue (P_{gran_per}). This is an important feature, because it is used as one of the indicators of the wound state. This feature is computed as follows:

  1. Once the tissues in the image have been labeled by the experts, a binary image is obtained by distinguishing between wound-bed (i.e. granulation, slough and necrosis) and *periulcer* (i.e. healing tissue and skin).
  2. The contour of the wound-bed area is computed.
  3. The number of pixels in the contour is calculated.
  4. The percentage of pixels in the wound-bed contour which are labeled as granulation gives us the descriptor P_{gran_per}.

- Ratio between granulation and devitalized tissues ($R_{gran-dev} = (1+A_{gran})/(1+A_{dev})$) (1 is added to both terms in the division to avoid indetermination). In this paper, it is considered as another indicator of the wound state.

- Ratio between wound-bed tissues and the whole PU (i.e. wound-bed + healing tissue) ($R_{wound-pu} = (1+A_{wound})/(1+A_{pu})$) (1 is again added to both terms in the division to avoid indetermination).

Finally, *differential descriptors* compute the variation between the same parameter in two one-week separated measures (t and $t-1$):

- One-week difference for all the absolute and relative features above, such as the areas of the different tissues ($\Delta A_{gran}(t) = A_{gran}(t) - A_{gran}(t-1)$,

$\Delta A_{slough}(t) = \ldots$, etc.) or the relative proportion of the tissues in the wound-bed ($\Delta P_{gran}(t) = P_{gran}(t) - P_{gran}(t-1)$, $\Delta P_{slough}(t) = \ldots$, etc.).

- Ratios between the one-week differences above and the absolute areas of reference for each tissue type ($R_{\Delta A_{gran}}(t) = \Delta A_{gran}(t)/(1 + A_{gran}(t-1))$, $R_{\Delta A_{slough}} = \ldots$, etc.). (1 is added to the denominator to avoid indetermination).

- Ratios between the one-week differences above and the wound-bed area ($R_{\Delta P_{gran}}(t) = \Delta A_{gran}(t)/(1 + A_{wound}(t-1))$, $R_{\Delta P_{slough}} = \ldots$, etc.). (1 is added to the denominator to avoid indetermination).

- Two specially important descriptors are: 1) the difference of proportion of granulation in the wound-bed perimeter, $\Delta P_{gran\_per}(t) = P_{gran\_per}(t) - P_{gran\_per}(t-1)$, and 2) the difference of ratio of granulation and devitalized tissues: $\Delta R_{gran-dev}(t) = R_{gran-dev}(t) - R_{gran-dev}(t-1)$. The signs of these two features are the variables to be predicted (see next subsection).

- One-week difference of the ratio between wound-bed area and PU area ($\Delta R_{wound-pu}(t) = R_{wound-pu}(t) - R_{wound-pu}(t-1)$).

2.3 Predicting the Wound State

Starting from the 46 features above, measured at two time instants, t (i.e. "this current week") and $t-1$ (i.e. "the week before"), giving a total 92 features, the predictive systems are designed to predict the sign, i.e. the positive (improvement) or negative (worsening) change, of these two differential parameters for PU evaluation, $\Delta P_{gran\_per}(\cdot)$ and $\Delta R_{gran-dev}(\cdot)$, at time $t+1$ (i.e. "next week").

To predict the sign of the change of wound-bed perimeter consisting of granulation tissue, the following binary function $S_1(t)$ is defined:

$$S_1(t) = \begin{cases} 1 & \text{if } \Delta P_{gran\_per}(t) > 0 \\ & \vee (\Delta P_{gran\_per}(t) = 0 \\ & \wedge \Delta P_{gran\_per}(t-1) < 0), \\ -1 & \text{otherwise} \end{cases} \quad (1)$$

In our database of 743 weekly-acquired PU images, 54% gave -1 and 46% gave 1 for this $S_1(t)$ function.

On the other hand, to predict the sign of the change of the granulation/devitalized ratio in the wound-bed, a similar binary function is used:

$$S_2(t) = \begin{cases} 1 & \text{if } \Delta R_{gran-dev}(t) > 0 \\ & \vee (\Delta R_{gran-dev}(t) = 0 \\ & \wedge \Delta R_{gran-dev}(t-1) < 0), \\ -1 & \text{otherwise} \end{cases} \quad (2)$$

In our database of 743 weekly-acquired PU images, 61% gave -1 and 39% gave 1 for this $S_2(t)$ function.

2.4 Machine Learning Approaches

Different supervised ML approaches have been used in this study to compare their performance for predicting the evolution of PUs. These approaches include *support vector machines* (SVM), *adaptive boosting* (AdaBoost), *linear discriminant analysis*, *naive Bayes classifiers*, *neural networks* (multi-layer perceptrons) and *decision trees*, but only a group of these approaches —SVMs, MLPs, Bayes classifiers and decision trees— gave us high performance results (accuracy $\sim 70\%$) when applied to our predictive problem.

On one hand, SVMs are a set of supervised-learning methods which have been successfully used in classification and regression problems. In classification tasks, such as tissue recognition on wound images, the SVMs work by building separation hyperplanes in the space, so that the margin between the different data classes is maximized (Drucker et al., 1997). On the other hand, naive Bayes classifiers are probabilistic classifiers based on the application of Bayes' theorem with strong independence assumptions, and have recently demonstrated their high efficiency rates in solving classification problems (Zhang, 2004). Multilayer perceptrons (MLP) are feed-forward networks with a set of sensory units (input neurons), one or more hidden layers of computation nodes and an output layer, which have been applied successfully to solve some difficult and diverse problem, such us pattern recognition, classification, regression or prediction, by training them with the back-propagation algorithm (Haykin, 1999). In the interests of this study, MLPs with one hidden layer

and a different number of neurons in this hidden layer have been used and tested. The results from the architectures which did the best for prediction are presented in next section (tables 1 and 2). Finally, a decision tree can be defined as a tree in which each internal node represents a choice between a number of alternatives, and each terminal node is marked by a classification. Decision trees are potentially powerful predictors and provide an explicit concept description for a dataset. Standard decision tree learners such as *C4.5* (Quinlan, 1993) expand nodes in depth-first order, while in *best-first decision tree* (BFT) learners the "best" node is expanded first (Shi, 2007). On the other hand, *alternating decision trees* (ADT) are a generalization of decision trees, voted decision trees and voted decision stumps, and use a learning algorithm that is based on boosting (Freund and Mason, 1999).

In this work, *RapidMiner* (Mierswa et al., 2006) has been used to do feature selection for each one of the ML approaches tested for prediction. The *FeatureSelection* operator of *RapidMiner* uses the two deterministic greedy feature selection algorithms, forward selection and backward elimination, but adds some enhancements to these standard algorithms. Moreover, k(=10)-folds stratified cross-validation has been used for this feature selection process.

3 RESULTS

In this section, performance results are presented from the machine-learning approaches which gave the best efficiency rates in predicting $S_1(t+1)$ and $S_2(t+1)$ (see equations 1 and 2), i.e. the sign of the change in one-week interval $(t+1)$ of our two descriptors designed for PU evaluation. Starting from 46 different input features (see section 2.2) at time t ("the current week") and $t-1$ ("a week ago"), i.e. 92 total input descriptors, feature selection (Mierswa et al., 2006) has been applied on each specific ML approach which has been implemented and tested as a predictive system of the future tendency (i.e. the sign) of our two variables that assess the wound state: 1) the proportion of wound-bed perimeter consisting of granulation tissue $\Delta P_{gran\_per}(t+1)$ (see equation 1) and 2) the ratio between granulation and devitalized tissue $\Delta R_{gran-dev}(t+1)$ (see equation 2). Feature selection significantly reduces the number of input descriptors for each one of the ML predictive systems designed. All these ML approaches were trained using both 10-fold and leave-one-out cross-validation strategies. The results from the leave-one-out cross-validation are shown in tables 1 and 2. (Training with 10-fold cross-validation gave us slightly higher per-

9

Table 1: Performance results from ML approaches with leave-one-out crossvalidation —Naive Bayes classifier, SVM, MLP with 2 neurons (h=2) in the hidden layer, and decision tree based algorithms (ADT, BFT and C4.5)— for predicting $S_1(t+1)$ (equation 1). The features resulting from the Feature Selection (FS) process are shown. Performance results shown are accuracy, sensitivity and positive predictive value (PPV) for both the two likely predicted signs of change (-1 and 1). See section 2.2 for notation.

ML Approach	FS	Accuracy	Sensitivity (-1)	Sensitivity (1)	PPV (-1)	PPV (-1)
Naive Bayes	$A_{wound}(t-1)$ $P_{gran\_per}(t-1)$ $R_{\Delta P_{gran\_per}}(t)$ $\Delta R_{gran-dev}(t)$	68.38%	76.81%	58.48%	68.47%	68.23%
SVM	$P_{dev}(t-1)$ $R_{gran-dev}(t-1)$ $R_{gran-dev}(t)$	68.38%	68.82%	67.86%	71.54%	64.96%
MLP (h=2)	$R_{gran-dev}(t-1)$ $R_{gran-dev}(t)$ $A_{gran}(t)$ $P_{dev}(t)$ $\Delta P_{dev}(t)$ $R_{\Delta A_{dev}}(t)$	72.07%	72.62%	71.43%	74.90%	68.97%
ADT	$A_{dev}(t)$ $\Delta R_{wound-pu}(t)$ $\Delta P_{gran\_per}(t)$	68.38%	62.36%	75.89%	76.82%	66.93%
BFT	$P_{gran\_per}(t-1)$ $A_{wound}(t)$ $A_{heal}(t)$ $P_{gran}(t)$ $R_{\Delta A_{gran}}(t)$ $\Delta R_{gran-dev}(t)$ $R_{\Delta P_{nec}}(t)$	74.13%	61.98%	88.39%	86.24%	66.44%
C4.5	$R_{gran-dev}(t-1)$ $A_{wound}(t)$ $P_{dev}(t)$	72.69%	64.64%	82.14%	80.95%	66.43%

formance results than the ones in these tables, but they are not shown here because k-fold cross-validation suffers from bias derived from the dataset split.)

3.1 Predicting Granulation in Perimeter

In table 1, the performance results from the ML approaches to predict $S_1(t+1)$ (see equation 1), i.e. the one-week increase or decrease in the proportion of granulation tissue in the wound-bed perimeter, are shown. The highest accuracy rate has been obtained with the BFT algorithm, but it needs the largest number of input parameters. As it is shown in table 1, C4.5 algorithm also achieves a high accuracy rate ($\sim 73\%$) with a reduced set of 3 input features. ADT is the only method which has not required any features at time $t-1$ in this experiment.

3.2 Predicting Granulation-Devitalized Ratio

In table 2, the performance results from the machine-learning approaches to predict $S_2(t+1)$ (see equation

2), i.e. the one-week increase or decrease in the ratio between granulation and devitalized tissue are shown. Decision trees with the C4.5 algorithm gave the best accuracy results (80.9%), with also very high sensitivity and positive predictive value rates obtained. It also uses a reduced number of 5 input parameters at t (i.e. features at $t-1$ are not needed in this case) to obtain these performance results of table 2. As in the case of predicting $S_1(t+1)$, ADT achieves good performance results with the most reduced input feature set.

4 CONCLUSIONS

Machine learning approaches to predict the evolution of PU have been designed and presented in this paper. These predictive systems have been based on the local characteristics extracted from digital PU images, which consisted of location and tissue area measurements. Images of a group of patients with hip or sacrum PUs were weekly taken in uncontrolled lighting conditions. These images were automatically seg-

Table 2: Performance results from ML approaches with leave-one-out crossvalidation —Naive Bayes, SVM, MLP with 4 neurons (h=4) in the hidden layer, and decision tree based algorithms (ADT, BFT and C4.5)— for predicting $S_2(t+1)$ (equation 2). The features resulting from the Feature Selection (FS) process are shown. Performance results shown are accuracy, sensitivity and positive predictive value (PPV) for both the two likely predicted signs of change (-1 and 1). See section 2.2 for notation.

ML Approach	FS	Accuracy	Sensitivity (-1)	Sensitivity (1)	PPV (-1)	PPV (-1)
Naive Bayes	$R_{wound-pu}(t-1)$ $A_{heal}(t)$ $P_{gran\_per}(t)$ $R_{\Delta A_{wound}}(t)$ $R_{\Delta P_{nec}}(t)$ $R_{wound-pu}(t)$ $\Delta P_{gran\_per}(t)$ $R_{\Delta P_{gran\_per}}(t)$	74.95%	87.29%	55.32%	75.65%	73.24%
SVM	$P_{dev}(t-1)$ $R_{gran-dev}(t-1)$ $P_{gran\_per}(t)$ $\Delta A_{nec}(t)$ $R_{\Delta P_{nec}}(t)$	75.98%	79.26%	70.74%	81.16%	68.21%
MLP (h=4)	$P_{gran}(t)$ $P_{nec}(t)$ $P_{gran\_per}(t)$ $\Delta P_{gran\_per}(t)$ $R_{\Delta P_{slough}}(t)$	77.82%	74.92%	82.45%	87.16%	67.39%
ADT	$A_{dev}(t)$ $A_{nec}(t-1)$ $R_{\Delta P_{gran\_per}}(t)$	75.15%	81.94%	64.36%	78.53%	69.14%
BFT	$\Delta P_{gran\_per}(t)$ $R_{\Delta A_{dev}}(t)$ $R_{\Delta P_{dev}}(t)$ $\Delta A_{slough}(t)$	76.39%	81.27%	68.62%	80.46%	69.73%
C4.5	$P_{gran\_per}(t)$ $R_{gran-dev}(t)$ $R_{\Delta P_{gran}}(t)$ $R_{\Delta P_{nec}}(t)$ $R_{\Delta P_{gran\_per}}(t)$	80.90%	77.56%	86.17%	89.92%	70.74%

mented by the mean shift procedure and manually labeled by a group of expert clinicians with the help of an *ad-hoc* intelligent graphical user interface for PU tissue classification. The after-one-week tendency of two different indicators for pressure ulcer evaluation is predicted: the ratio between granulation and devitalized tissue, and the percentage of wound-bed border consisting of granulation tissue.

Of the tens of machine learning approaches and architectures tested in this study, support vector machines, naive Bayes classifiers, neural networks and decision trees achieved the highest accuracy rates in the prediction of those two PU-state indicators, giving also acceptable sensitivity and positive predictive value rates. Feature selection significantly reduced the number of input features needed for prediction. Decision trees gave the best performance results, as the C4.5 algorithm achieved the highest accuracy rate ($\sim 81\%$) in the prediction of the granulation/devitalized ratio from a small number of input

features. Finally, multi-layer perceptrons also showed their appropriateness for these prediction tasks and gave performance rates similar to the ones obtained with decision trees.

These results show that predicting the positive or negative tendency of the changes in the proportion or location of wound tissues can be reliably achieved by machine learning approaches such as decision trees or neural networks. Clinicians are now supplied with a predictive tool which can be used to estimate the evolution of pressure ulcers and helps the effective management of health resources and planning of pharmacological treatment and health-care decisions.

ACKNOWLEDGEMENTS

REFERENCES

Comaniciu, D. and Meer, P. (2002). Mean shift: A robust approach toward feature space analysis. *IEEE Trans. Pattern Analysis Machine Intell.*, 24(5):603–619.

Dowsett, C. (2008). Using the TIME framework in wound bed preparation. *Br J Community Nurs*, 13(6):S15–6, S18, S20 passim.

Drucker, H., Burges, C. J., Kaufman, L., Smola, A., and Vapnik, V. (1997). Support vector regression machines. *Advances in Neural Information Processing Systems*, 9:155–161.

Edsberg, L. E. (2007). Pressure ulcer tissue histology: An appraisal of current knowledge. *Ostomy/Wound Management*, 53(10):40–49.

European Pressure Ulcer Advisory Panel (EPUAP) (1999). Guidelines on treatment of pressure ulcers. *EPUAP Review*, 1:31–33.

Freund, Y. and Mason, L. (1999). The alternating decision tree algorithm. In *Proceedings of the 16th International Conference on Machine Learning*.

Gawlitta, D., Li, W., Oomens, C. W. J., Baaijens, F. P. T., Bader, D. L., and Bouten, C. V. C. (2007). The relative contributions of compression and hypoxia to development of muscle tissue damage: An in vitro study. *Annals of Biomedical Engineering*, 35(2):273–284.

Günes, U. Y. (2009). A prospective study evaluating the Pressure Ulcer Scale for Healing to assess stage II, stage III, and stage IV pressure ulcers. *Ostomy Wound Management*, 55(5):48–52.

Gunningberg, L. (2004). Risk, prevalence and prevention of pressure ulcers in three swedish healthcare settings. *Journal of Wound Care*, 13(7):286–290.

Haykin, S. (1999). *Neural networks a comprehesive foundation*. Prentice Hall, New Jersey, USA, second edition.

Horn, S. D., Bender, S. A., Bergstrom, N., Cook, A. S., Ferguson, M. L., Rimmasch, H. L., Sharkey, S. S., Smout, R. J., Taler, G. A., and Voss, A. C. (2002). Description of the national pressure ulcer long-term care study. *Journal of the American Geriatrics Society*, 50(11):1816–1825.

Kottner, J., Raeder, K., Halfens, R., and Dassen, T. (2009). A systematic review of interrater reliability of pressure ulcer classification systems. *Journal of Clinical Nursing*, 18(3):315–336.

Landi, F., Onder, G., Russo, A., and Bernabei, R. (2007). Pressure ulcer and mortality in frail elderly people living in community. *Archives of Gerontology and Geriatrics*, 44(Supplement 1):217 – 223.

Mierswa, I., Wurst, M., Klinkenberg, R., Scholz, M., and Euler, T. (2006). Yale: Rapid prototyping for complex data mining tasks. In Ungar, L., Craven, M., Gunopulos, D., and Eliassi-Rad, T., editors, *KDD '06: Proceedings of the 12th ACM SIGKDD International Conference on Knowledge Discovery and Data Mining*, pages 935–940, New York, NY, USA. ACM.

National Pressure Ulcer Advisory Panel, Cuddigan, J., Ayello, E., and Sussman, C., editors (2001). *Pressure ulcers in America: Prevalence, incidence, and implications for the future*. Reston, VA: NPUAP.

Quinlan, R. (1993). *C4.5: Programs for Machine Learning*. Morgan Kaufmann Publishers.

Redelings, M. D., Lee, N. E., and Sorvillo, F. (2005). Pressure ulcers: More lethal than we thought? *Advances in Skin & Wound Care*, 18(7):367–372.

Shi, H. (2007). *Best-first decision tree learning*. PhD thesis, University of Waikato, Hamilton, NZ. COMP594.

Stratton, R., Green, C., and Elia, M. (2003). *Disease-related Malnutrition: An evidence-based approach to treatment*. CABI Publishing, Wallingford, United Kingdom.

Sussman, C. and Bates-Jensen, B., editors (2001). *Wound Care: A Collaborative Practice Manual for Physical Therapists and Nurses*. Lippincott Williams & Wilkins.

Tannen, A., Dassen, T., Bours, G., and Halfens, R. (2004). A comparison of pressure ulcer prevalence: concerted data collection in the netherlands and germany. *International Journal of Nursing Studies*, 41(6):607–612.

Veredas, F. J., Mesa, H., and Morente, L. (2009). A hybrid learning approach to tissue recognition in wound images. *International Journal of Intelligent Computing and Cybernetics*, 2(2):327–347.

Wannous, H., Treuillet, S., and Lucas, Y. (2007). Supervised tissue classification from color images for a complete wound assessment tool. In *Proceedings of the 29th Annual International Conference of the IEEE EMBS*, pages 6031–6034, Cit Internationale, Lyon, France.

Woodbury, M. and Houghton, P. (2004). Prevalence of pressure ulcers in canadian healthcare settings. *Ostomy Wound Management*, 50(10):22–38.

Zhang, H. (2004). The optimality of Nave Bayes. In *Proc. 17th Internat. FLAIRS Conf.*, pages 562–567, Florida, USA.

Zulkowski, K. (1999). MDS+ items not contained in the pressure ulcer RAP associated with pressure ulcer prevalence in newly institutionalized elderly. *Ostomy Wound Management*, 45(1):24–33.